

# The Herpes Simplex Virus 1 IgG Fc Receptor Blocks Antibody-Mediated Complement Activation and Antibody-Dependent Cellular Cytotoxicity *In Vivo*<sup>∇</sup>

John M. Lubinski, Helen M. Lazear,<sup>†</sup> Sita Awasthi, Fushan Wang, and Harvey M. Friedman\*

*Division of Infectious Disease, Department of Medicine, University of Pennsylvania School of Medicine, Philadelphia, Pennsylvania 19104-6073*

Received 1 December 2010/Accepted 4 January 2011

**Herpes simplex virus 1 (HSV-1) glycoprotein E (gE) mediates cell-to-cell spread and functions as an IgG Fc receptor (FcγR) that blocks the Fc domain of antibody targeting the virus or infected cell. Efforts to assess the functions of the HSV-1 FcγR *in vivo* have been hampered by difficulties in preparing an FcγR-negative strain that is relatively intact for spread. Here we report the FcγR and spread phenotypes of NS-gE264, which is a mutant strain that has four amino acids inserted after gE residue 264. The virus is defective in IgG Fc binding yet causes zosteriform disease in the mouse flank model that is only minimally reduced compared with wild-type and the rescue strains. The presence of zosteriform disease suggests that NS-gE264 spread functions are well maintained. The HSV-1 FcγR binds the Fc domain of human, but not murine IgG; therefore, to assess FcγR functions *in vivo*, mice were passively immunized with human IgG antibody to HSV. When antibody was inoculated intraperitoneally 20 h prior to infection or shortly after virus reached the dorsal root ganglia, disease severity was significantly reduced in mice infected with NS-gE264, but not in mice infected with wild-type or rescue virus. Studies of C3 knockout mice and natural killer cell-depleted mice demonstrated that the HSV-1 FcγR blocked both IgG Fc-mediated complement activation and antibody-dependent cellular cytotoxicity. Therefore, the HSV-1 FcγR promotes immune evasion from IgG Fc-mediated activities and likely contributes to virulence at times when antibody is present, such as during recurrent infections.**

Herpes simplex virus 1 (HSV-1) encodes a receptor for the Fc domain of IgG (FcγR) (57). The HSV-1 FcγR is expressed on the viral envelope and at the surface of infected cells (4, 44, 45). HSV-1 glycoprotein E (gE) forms a heterodimeric complex with glycoprotein I (gI) that binds the Fc domain of IgG at a higher affinity than gE alone (5, 9, 17, 25, 48). HSV-1 gI alone fails to function as an FcγR (5, 17). The HSV-1 FcγR participates in immune evasion by promoting antibody bipolar bridging, which refers to the IgG Fab domain of HSV antibody binding to its target antigen while the Fc domain of the same antibody molecule binds to the HSV-1 FcγR (18, 20, 42, 55). The concept of antibody bipolar bridging was supported by resolving the crystal structure of the HSV-1 FcγR bound to IgG Fc (53).

Functions assigned to the IgG Fc domain include activation of the classical complement pathway and binding to immune effector cells that express FcγRs. *In vitro* studies to address the functions of the HSV-1 FcγR have demonstrated that the FcγR protects the virus from antibody-dependent complement neutralization, antibody-dependent cellular cytotoxicity (ADCC), and Fc-mediated attachment of granulocytes to HSV-1-infected cells (18, 20, 42, 55). However, *in vivo* studies of HSV-1 FcγR function have been hampered by difficulties in

producing a HSV-1 gE mutant strain that is defective in FcγR function but in which other gE-mediated activities are intact.

HSV-1 gE is required for efficient spread of virus from one epithelial cell to another and from epithelial cells to neurons (14, 15, 39, 47, 49, 56, 58). HSV-1 gE also mediates targeting of capsid, tegument, and viral glycoproteins from the neuron cell body into axons (56). Partially overlapping gE domains mediate FcγR activity and spread, posing a challenge to separate these functions (42, 47, 58). *In vivo* studies have also been hampered by the observation that the HSV-1 FcγR binds the Fc domain of human IgG, but not murine or guinea pig IgG (24). Although the IgG Fc domain of rabbit IgG binds to the HSV-1 FcγR, the best-defined HSV-1 rabbit model is HSV-1 keratitis (6). This model is not optimal for evaluating the function of the HSV-1 FcγR, since the cornea is an avascular structure and low titers of IgG are present in tears (50).

The biologic relevance of the HSV-1 FcγR cannot be evaluated in mice or guinea pigs unless the animal models are modified. The murine flank model was modified by passively immunizing animals with human IgG antibody to HSV (human immune IgG) prior to HSV-1 infection (34, 42). The results demonstrated a role for the HSV-1 FcγR in virulence at the inoculation site; however, the study was limited by the fact that HSV-1 FcγR-defective gE mutant strain NS-gE339 was impaired in causing zosteriform disease because the mutant virus was defective in spread activity (42). Here, we define the FcγR and spread phenotypes of a previously reported HSV-1 mutant, NS-gE264, and demonstrate that it is capable of causing zosteriform disease that is only minimally impaired compared with wild-type and rescue strains (56). In the murine flank model, human IgG antibody to HSV reduced the severity of

\* Corresponding author. Mailing address: 502 Johnson Pavilion, University of Pennsylvania, Philadelphia, PA 19104-6073. Phone: (215) 573-8432. Fax: (215) 349-5111. E-mail: hfriedma@mail.med.upenn.edu.

<sup>†</sup> Present address: 660 S. Euclid Ave., Campus Box 8051, St. Louis, MO 63110.

<sup>∇</sup> Published ahead of print on 12 January 2011.

zosteriform disease caused by the mutant strain while having no effect on wild-type or rescue virus. The HSV-1 Fc $\gamma$ R protected the virus by blocking IgG Fc-mediated complement activation and NK cell-mediated ADCC *in vivo*.

## MATERIALS AND METHODS

**Cells.** Vero (African green monkey kidney epithelial) cells and HaCaT (human keratinocyte) cells were propagated in Dulbecco's modified Eagle's medium (DMEM) supplemented with 10 mM HEPES (pH 7.3), 2 mM L-glutamine, 20  $\mu$ g/ml gentamicin, and 5% heat-inactivated fetal bovine serum (FBS). HaCaT cells were maintained at confluence for 3 to 4 days to allow them to polarize prior to infection (39).

**Viruses.** HSV-1 strain NS is a low-passage clinical isolate (21). NS-gEnull contains the *lacZ* gene under the control of the HSV-1 ICP6 promoter, with gE amino acids 124 to 512 replaced, and produces no functional gE protein (42, 56). NS-gE264 was constructed as previously described and contains an XhoI linker that results in the insertion of four amino acids after gE residue 264, based on the sequence of HSV-1 strain 17. The linker insertion is actually after gE amino acid 266 in HSV-1 strain NS, which has two additional amino acids at gE positions 186 and 187 compared to strain 17 (16, 56). A rescue virus (rNS-gE264) was constructed by cotransfection of NS-gE264 viral DNA with pCMV3-gE containing the entire gE coding sequence. Recombinants were selected by PCR amplification of gE DNA and screening for loss of the XhoI restriction site. The rescue strain was plaque purified three times. Virus stocks were prepared by infecting Vero cells at a multiplicity of infection (MOI) of 0.01 and collecting the infected cells and media when the cytopathic effect reached 100%. Campenot chamber and mouse retina infections used virus that was purified on a sucrose gradient and resuspended in phosphate-buffered saline (PBS) (39). Virus titers were determined by plaque assay on Vero cells.

**Mouse strains.** BALB/c mice were purchased from the National Cancer Institute, and C57BL/6 mice were purchased from Jackson Laboratory. C3 knockout mice homozygous for depletion in the complement C3 gene were originally obtained from Richard Wetsel (University of Texas) and bred at the University of Pennsylvania under IACUC guidelines (35).

**Antibodies.** Human IgG antibody to HSV was purchased from the Michigan Department of Public Health, Lansing, MI, and contained high titers of antibody to HSV-1 and HSV-2. The IgG was prepared from sera of thousands of HIV-negative blood donors (42). Murine IgG antibody to HSV-1 (murine immune IgG) was purified from sera of mice infected by flank scarification with HSV-1 NS and bled 2 to 3 weeks postinfection. Polyclonal rabbit anti-HSV-1 (Dako), UP575 anti-gE, UP1928 anti-gI, and NC-1 anti-VP5 and murine monoclonal antibody (MAb) Fd69 anti-gI have been previously described (3, 12, 22, 31, 40, 56). Antiactin MAb C4 was obtained from MP Biomedicals, while rat anti-mouse Thy1.2 (PharMingen) was used as a neuronal cell marker. Secondary antibodies used were Alexa-555 goat anti-rabbit, Alexa-488 donkey anti-rat (Invitrogen), horseradish peroxidase (HRP) anti-mouse, and HRP anti-rabbit (GE Healthcare) antibodies. Anti-NK1.1 (PK136) and CL18 (isotype control) were used to deplete NK cells (Bio X Cell) (27, 52).

**Western blotting and immunoprecipitation.** Infected Vero cell extracts were treated with 1% Triton X-100, the nuclei were pelleted, and the supernatant fluids were stored at  $-80^{\circ}\text{C}$  until testing. Immunoprecipitation was performed by incubating cell extracts with anti-gI MAb Fd69 and protein G-agarose beads (Invitrogen). Cell extracts and immunoprecipitates were separated by SDS-PAGE on 4-to-15% Tris-HCl gels (Bio-Rad), transferred to Immobilon P membranes, and probed with the indicated antibodies. Blots were incubated with enhanced chemiluminescence substrate (GE Healthcare) and imaged on X-Omat film (Kodak).

**Complement-enhanced antibody neutralization.** For complement-enhanced antibody neutralization, approximately  $10^5$  PFU of NS-gE264 or the rescue virus was incubated for 1 h at  $37^{\circ}\text{C}$  in 100  $\mu$ l of DMEM containing 10% FBS and 5% HSV-1 and HSV-2 antibody-negative human serum as the source of complement, or human IgG antibody to HSV at 50  $\mu$ g/ml as the source of antibody, or 50  $\mu$ g/ml of human IgG antibody to HSV and 5% human complement as sources of antibody and complement. Murine IgG antibody to HSV-1 at 12.5  $\mu$ g/ml was used in some neutralization experiments.

**FACS analysis of infected cells.** For fluorescence-activated cell sorting (FACS) analysis, Vero cells were infected at an MOI of 2 to 5 for 16 h and treated with 0.25 U/ml of neuraminidase for 30 min at  $37^{\circ}\text{C}$  (31, 42). Surface expression of the HSV-1 Fc $\gamma$ R was detected using 10  $\mu$ g/ml biotinylated HSV-1 and HSV-2 non-immune human IgG, while gE expression was evaluated using 1  $\mu$ g/ml anti gE MAb 1BA10 added for 1 h at  $4^{\circ}\text{C}$  followed by streptavidin-phycoerythrin-con-

jugated or fluorescein isothiocyanate-conjugated anti-mouse IgG for 1 h at  $4^{\circ}\text{C}$ . Analysis was performed using a BD FACSCalibur and CellQuest Pro software.

**Plaque sizes.** For determination of plaque sizes, confluent HaCaT cells were infected with approximately 50 PFU in 12-well plates, overlaid with 0.6% low-melt agarose, and stained with neutral red. Plaque areas were calculated at 72 h by measuring two perpendicular diameters by using an eyepiece micrometer at  $40\times$  magnification (39, 49).

**Infection of SCG neurons in Campenot chambers.** Superior cervical ganglia (SCG) neurons were cultured in Campenot chambers (10, 11, 38, 39). Dissociated neurons from half a SCG were seeded into the soma (S) chamber and cultured for 2 to 3 weeks until extensive neurite (axon) growth was observed in the neurite (N) chamber. One day prior to infection, the middle (M) chamber was filled with neuron medium containing 1% methylcellulose. For anterograde spread experiments, Vero cells were mixed 1:1 with medium and added to the N chamber 1 day prior to infection at a density sufficient to produce a confluent monolayer the next day. A total of  $1 \times 10^5$  PFU was added to the S chamber for 1 h at  $37^{\circ}\text{C}$ . At 48 h postinfection, cells and supernatant fluids in the N and S chambers were harvested for determinations of viral titers. For retrograde spread experiments, HaCaT cells were added to the N chamber and allowed to reach confluence for 3 to 4 days prior to infection. A total of  $1 \times 10^5$  PFU was added to the N chamber for 1 h at  $37^{\circ}\text{C}$ , and then the inoculum was removed and medium containing 1% methylcellulose was added to the N chamber. At 48 h postinfection, the cells and supernatant fluids in the N and S chambers were harvested for determinations of viral titer.

**Mouse retina infection.** For the mouse retina infection experiment, 8- to 9-week-old BALB/c mice were inoculated with 1  $\mu$ l containing  $4 \times 10^5$  PFU (38, 56). Mice were sacrificed 5 days postinfection, and eyes were cut in 10- $\mu$ m sections for immunofluorescence analysis in the saggital plane and mounted directly on slides that were heated at  $45^{\circ}\text{C}$  for 30 min prior to staining. Retinas were incubated with rabbit anti-HSV-1 and rat anti-Thy1.2, followed by Alexa-555 anti-rabbit and Alexa-488 anti-rat secondary antibodies. Nuclei were stained with 4',6-diamidino-2-phenylindole (DAPI; Invitrogen). Slides were mounted with Pro-Long Gold antifade reagent (Invitrogen) and viewed under a Nikon Eclipse E1000 microscope with a BW Evolution QE camera. Brains were cut in 40- $\mu$ m sections in the coronal plane and transferred to cryoprotectant solution (30% sucrose, 30% ethylene glycol, 1% polyvinylpyrrolidone in PBS). Tissues were stored at  $-20^{\circ}\text{C}$  until staining. Immunohistochemistry was performed on brain sections using rabbit anti-HSV-1 IgG and avidin-biotin complex. Sections were counterstained with cresyl violet and viewed under a Nikon Eclipse E1000 microscope with a Color Insight QE camera. Images were processed using Phase 3 imaging software and Adobe Photoshop.

**Murine flank model.** For the murine flank model experiments, BALB/c mice were anesthetized and the hair was removed (34, 35, 42). Nonimmune human IgG or human IgG antibody to HSV was passively transferred intraperitoneally (i.p.) in 100  $\mu$ l DMEM. Twenty hours later, 10  $\mu$ l of virus was applied to the flank by scratch inoculation. Zosteriform disease was scored as follows: individual lesions separate from the inoculation site were each given a score of 1 to a maximum value of 10. To deplete NK cells, C57BL/6 mice were inoculated i.p. three times with 100  $\mu$ g of PK136 (anti-NK1.1) or CL18 (mouse IgG2A isotype control) 1 day prior to infection and 2 and 5 days postinfection (27, 52).

**Quantitation of virus in murine DRG.** For quantitation of virus, at the indicated times dorsal root ganglia (DRG) from the infected side were harvested and titers were determined by plaque assay on Vero cells (7).

**Statistical analysis.** All statistical analyses were performed with GraphPad Prism software. One-way analysis of variance (ANOVA) followed by Tukey's multiple comparison test was used for the results shown below in Fig. 2 and 5, and a two-way ANOVA with Bonferroni post tests was used for the results shown below in Fig. 6 to 8.

## RESULTS

**gE264 forms a complex with gI.** The expression of gE and gI and the ability of gE to form a complex with gI were evaluated by infecting Vero cells with NS-gE264 or with HSV-1 strains NS, NS-gEnull, and rNS-gE264 as controls (Fig. 1). NS-gE264 expresses gE and gI, although at reduced levels and with diminished glycosylation compared with the rescue and wild-type strains; however, as discussed below, gE and gI expression levels are sufficient to maintain relatively intact spread activities *in vivo*. HSV-1 gE coimmunoprecipitated with gI from

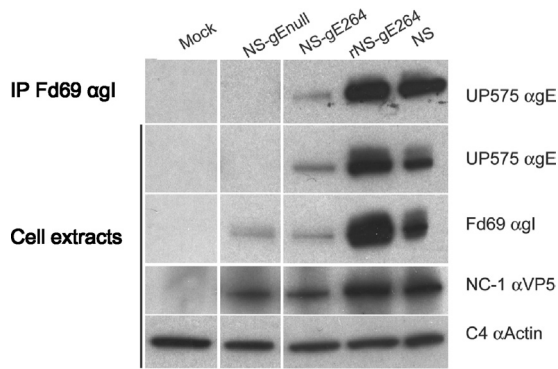


FIG. 1. Characterization of NS-gE264. Immunoprecipitation (IP) of cell extracts using anti-gI MAb Fd69 were prepared from mock-infected or HSV-1-infected Vero cells (top row) and probed by Western blotting with anti-gE UP575. Mock or infected cell extracts (next four rows) were probed by Western blotting with the indicated antibodies. All lanes shown are from the same gel, but lanes containing irrelevant samples were cropped from the image.

NS-gE264-infected cells, indicating that the mutation at residue 264 does not disrupt the interaction between gE and gI.

**Spread phenotype of NS-gE264 *in vitro*.** We previously determined that NS-gE264 antigens were detected in axons of SCG

neurons by immunofluorescence by using a polyclonal anti-HSV antibody *in vitro* (56). Here, the Campenot chamber system was used to more fully assess spread in the anterograde and retrograde directions and to quantify differences between the mutant and wild-type strains (Fig. 2A) (10, 11, 38, 39). To evaluate anterograde spread, neuron cell bodies in the S chamber were infected with NS-gE264 or rNS-gE264 and the titers were determined for the contents of the N and S chambers 48 h postinfection. The two viruses produced similar titers in the S chamber, indicating similar input titers and replication in S chamber neurons; however, NS-gE264 titers in the N chamber were approximately 1 log<sub>10</sub> lower than the rescue virus (Fig. 2B), supporting a partial defect in anterograde spread for NS-gE264.

To evaluate retrograde spread, NS-gE264 or rNS-gE264 was added to HaCaT cells in the N chamber, and titers were determined for the contents of the N and S chambers 36 h postinfection (39). No significant difference was detected in N chamber titers, indicating comparable replication in HaCaT cells. Importantly, S chamber titers were similar for the two viruses (Fig. 2C), supporting intact retrograde spread. In addition, no significant difference in S chamber titers was detected when N chamber neurites were infected in the absence of HaCaT cells (data not shown), which supports intact retrograde transport of NS-gE264.

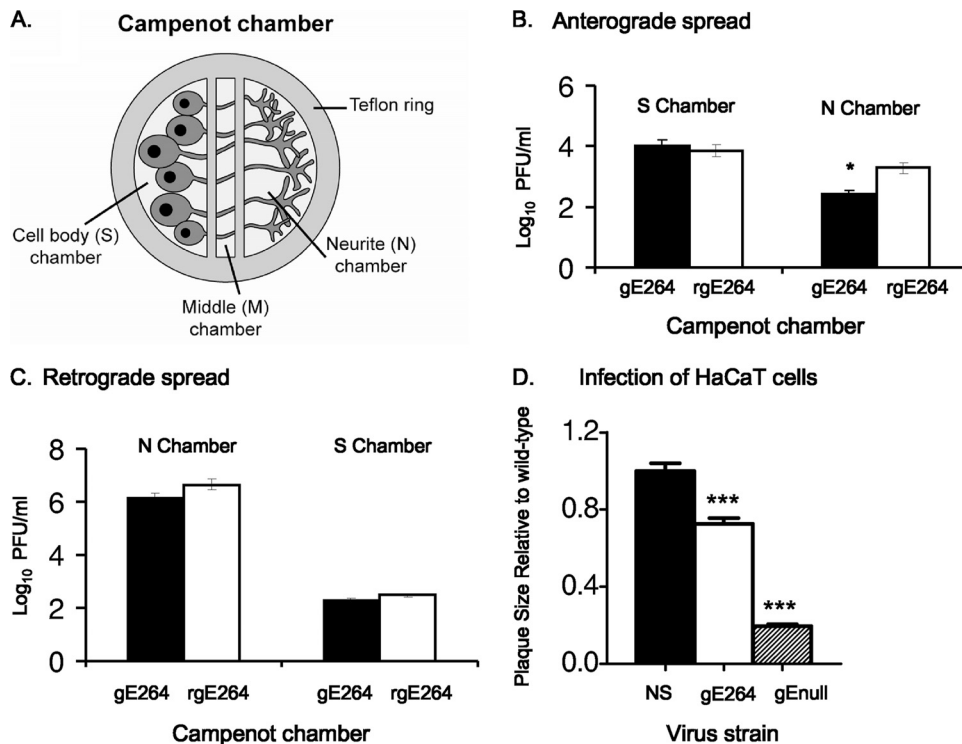


FIG. 2. Spread phenotype of NS-gE264 *in vitro*. (A) Cartoon of the Campenot chamber system. A Teflon ring is placed on silicon grease within a tissue culture dish to divide the culture into three compartments. SCG neurons are added to the cell body (S) chamber. Neurites (axons) grow through the silicon barrier into the middle (M) and neurite (N) chamber over 2 to 3 weeks. (B) A total of  $1 \times 10^5$  PFU NS-gE264 or rNS-gE264 was added to S chamber neurons. The titers for the contents of the S and N chambers were determined on Vero cells 48 h postinfection. Results shown are the means  $\pm$  standard errors of five chambers. \*,  $P < 0.05$ . (C) HaCaT cells were added to N chamber neurites 1 week prior to infection. A total of  $1 \times 10^5$  PFU of NS-gE264 or rNS-gE264 was added to the N chamber and overlaid with methylcellulose following infection. The titers of the contents of the N and S chambers were determined on Vero cells 36 h postinfection. Results are the means  $\pm$  standard errors of six chambers. (D) Plaque sizes of NS and NS-gE264 viruses in HaCaT cells. Results are the means  $\pm$  standard errors of an experiment that counted 30 to 40 plaques. \*\*\*,  $P < 0.001$ , comparing NS-gE264 with NS or NS-gEnull. gE-264 is strain NS-gE264; gEnull is strain NS-gEnull.

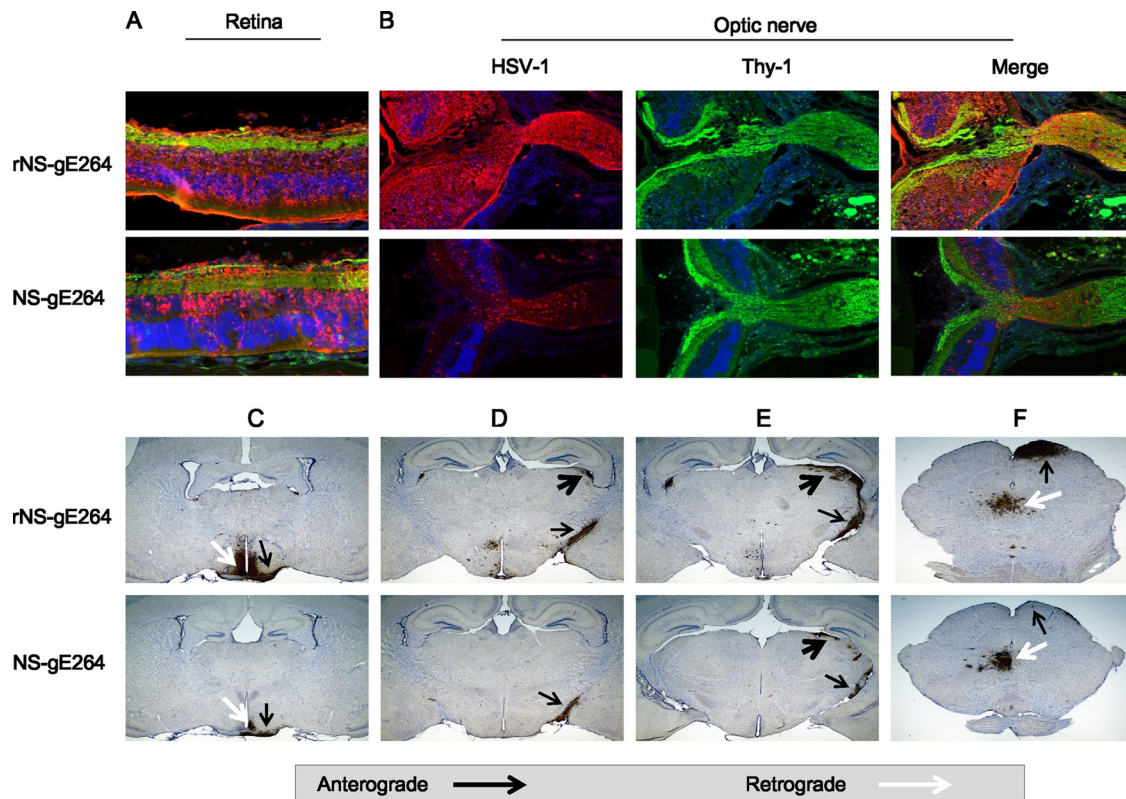


FIG. 3. Spread phenotype of NS-gE264 in the mouse retina model. Mice were infected with  $4 \times 10^5$  PFU rNS-gE264 ( $n = 3$ ) or NS-gE264 ( $n = 5$ ), and tissues were harvested 5 days postinfection. Sections were stained by immunofluorescence with anti-HSV-1 IgG (red), the neuronal marker anti-Thy1 (green), and DAPI (blue). (A) Sections of retina showing multiple cell layers extending from ganglion cell neurons, shown in green at the top of each image, to retina pigmented epithelial cells, shown in red at the bottom of each image. Magnification,  $\times 200$ . (B) The retina, rotated  $90^\circ$  counterclockwise compared with the image shown in panel A, is shown on the left side of each image, while the optic nerve at the exit site from the retina is shown on the right. Magnification,  $\times 100$ . (C) Anterograde transport to the optic tract (black arrows) and multisynaptic retrograde spread to the suprachiasmatic nucleus (white arrows). (D and E) Anterograde axonal transport to the optic tract (black arrows) and anterograde spread to the lateral geniculate nucleus (black arrowheads). (F) Anterograde spread to the superior colliculus (black arrows) and retrograde spread to the oculomotor and Edinger-Westphal nuclei (white arrows). Magnification in panels C to F,  $\times 20$ .

Plaque size in HaCaT cells was evaluated to assess epithelial cell-to-cell spread. NS-gE264 produced plaques that were approximately 25% smaller than wild-type plaques; however, the NS-gE264 plaques were significantly larger than plaques produced by NS-gE $\Delta$ , which fails to encode a gE protein (Fig. 2D), indicating a partial cell-to-cell spread defect for NS-gE264.

**Spread phenotype of NS-gE264 *in vivo*.** NS-gE264 spread *in vivo* was evaluated in the mouse retina infection model. We previously reported that NS-gE264 produced extensive retinal infection and that viral antigens were detected in the optic nerve, consistent with intact anterograde spread (56). A more detailed analysis was performed by comparing retinal infection of NS-gE264 versus that with rNS-gE264 and evaluating spread to the brain. Both viruses showed extensive retina infection (Fig. 3A) and anterograde axonal transport of viral proteins into the optic nerve (Fig. 3B), although NS-gE264 antigens were diminished in the retina and optic nerve compared with the rescue strain. Both viruses spread along anterograde and retrograde pathways to the brain (Fig. 3C to F); however, NS-gE264 anterograde spread was reduced compared with the rescue virus. Based on the retina infection model, SCG neuron cultures, and plaque sizes, we conclude that NS-gE264 is par-

tially impaired in cell-to-cell and anterograde spread, with no impairment in retrograde spread.

**NS-gE264 expresses gE at the cell surface and is defective in Fc $\gamma$ R activity.** We previously reported that cells infected with NS-gE264 do not form rosettes with IgG-coated erythrocytes, which indicates that the mutant strain does not express the lower-affinity Fc $\gamma$ R formed by gE (17). Vero cells were infected with NS-gE264, or NS, rNS-gE264, and NS-gE $\Delta$  as controls, to assess the level of expression of gE at the infected cell surface and determine whether NS-gE264-infected cells form the higher-affinity Fc $\gamma$ R produced by the gE/gI complex (Fig. 4A to D) (17). NS- and rNS-gE264-infected cells expressed gE at the cell surface and an Fc $\gamma$ R that bound monomeric nonimmune human IgG (Fig. 4A and B). The NS-gE $\Delta$  mutant strain did not express gE or the higher-affinity Fc $\gamma$ R (Fig. 4C). NS-gE264 expressed gE at the cell surface, although at slightly lower levels than NS or the rescue strain, and was almost totally defective in binding nonimmune human IgG (Fig. 4D).

**NS-gE264 is more susceptible to complement-enhanced antibody neutralization.** We postulated that NS-gE264 would be more susceptible than the rescue strain to complement-enhanced antibody neutralization, because the IgG Fc domain is

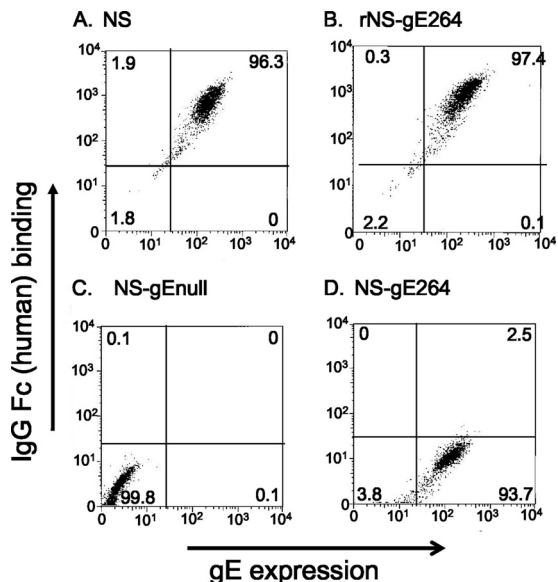


FIG. 4. HSV-1 Fc $\gamma$ R activity. Vero cells were infected at an MOI of 2 to 5 with the indicated viruses. HSV-1 gE expression on the cell surface was detected with MAb 1BA10, and IgG Fc binding was evaluated using biotin-labeled nonimmune human IgG. The percentages of positive cells are indicated in the quadrants.

available to activate complement (Fig. 5A). Viruses were incubated with (i) 5% human complement, (ii) human IgG antibody to HSV at a concentration that neutralizes by ~50% (50  $\mu$ g/ml), or (iii) antibody and complement (Fig. 5B). The rNS-gE264 strain was neutralized to 0.3 log<sub>10</sub> by antibody alone compared with 0.4 log<sub>10</sub> by antibody and complement. In contrast, NS-gE264 was neutralized to 0.2 log<sub>10</sub> by antibody alone and 1.6 log<sub>10</sub> by antibody and complement. Neither strain was neutralized by complement alone. Therefore, the inability of NS-gE264 to bind the Fc domain of antibody renders the virus significantly more susceptible to complement-enhanced antibody neutralization.

We postulated that murine antibody and complement would have similar neutralizing activities against NS-gE264 and the rescue strain, since the HSV-1 Fc $\gamma$ R does not bind the Fc domain of murine IgG (24). NS-gE264 or rNS-gE264 was incubated with (i) 5% human complement, (ii) murine IgG antibody to HSV-1 at a concentration that neutralizes by ~50% (12.5  $\mu$ g/ml), or (iii) antibody and complement (Fig. 5C). The titers of both virus strains were significantly reduced by antibody and complement, with a slightly greater effect on the rescue strain than NS-gE264. The results indicated that the ability of the gE/gI complex to bind the Fc domain of human

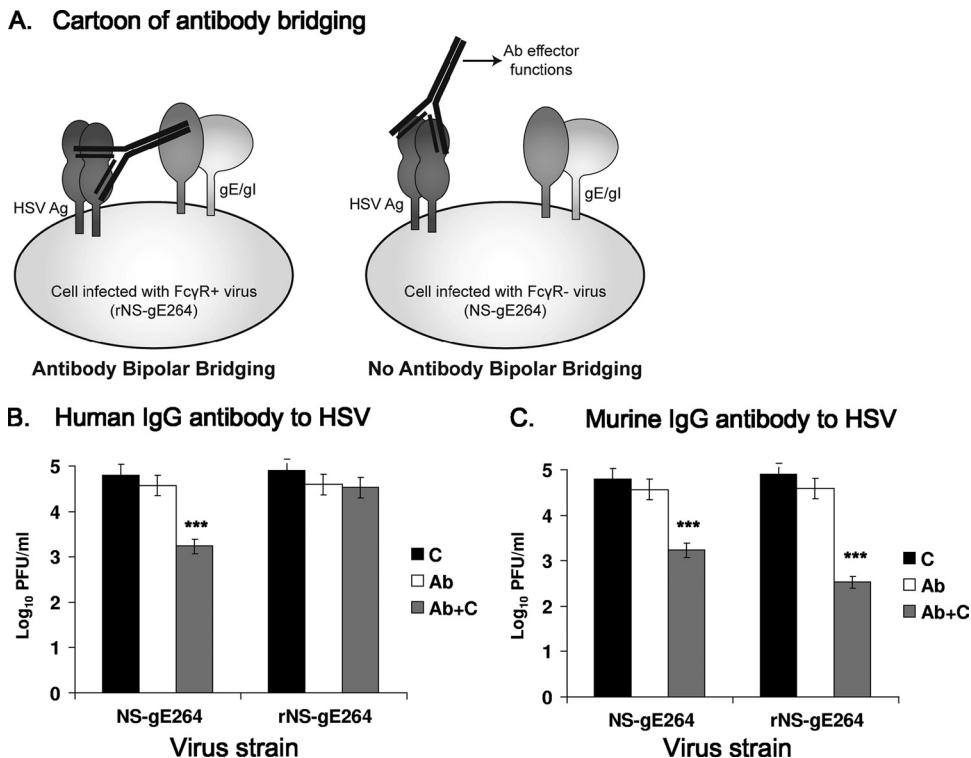


FIG. 5. Antibody-dependent complement neutralization. (A, left) HSV-1 IgG antibody binds to HSV-1 antigen by the Fab domain, and the Fc domain of the same antibody molecule binds to the HSV-1 Fc $\gamma$ R (gE/gI). (Right) The cell is infected with NS-gE264, which expresses gE/gI but fails to form an Fc $\gamma$ R. HSV-1 IgG antibody binds to HSV-1 antigen by the Fab domain, but the Fc domain fails to bind to the Fc $\gamma$ R (gE/gI). (B) NS-gE264 and rNS-gE264 were incubated with 5% human serum as a source of complement (C) from an HSV-1- and HSV-2-seronegative donor, or incubated with human IgG antibody to HSV (Ab) at a concentration that neutralizes virus by ~50%, or with antibody and complement (Ab+C). \*\*\*,  $P < 0.001$  for comparison of Ab+C with Ab alone or C alone. (C) NS-gE264 and rNS-gE264 were incubated with human complement as described above, or with murine IgG antibody to HSV-1, or with antibody and complement. \*\*\*,  $P < 0.001$  for comparison of Ab+C with Ab alone or C alone for NS-gE264 and rNS-gE264. Results in panels B and C are the means and standard deviations of three experiments.

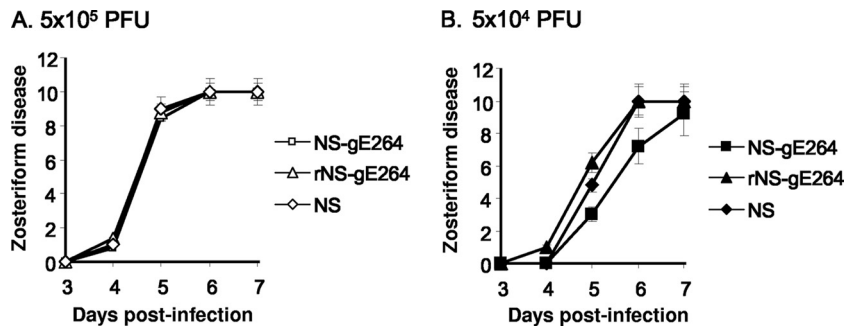


FIG. 6. Zosteriform disease scores obtained in the mouse flank model. Mice were scratch inoculated on the flank with NS-gE264, rNS-gE264, or NS at  $5 \times 10^5$  PFU (A) or  $5 \times 10^4$  PFU (B) and scored for zosteriform disease. Results represent 10 mice in each group  $\pm$  the standard deviation. Curves were not significantly different ( $P > 0.05$ ).

IgG antibody to HSV protects the virus from complement-enhanced antibody neutralization.

**NS-gE264 produces zosteriform disease comparable to that produced by wild-type and rescue strains.** The mouse flank model is useful for assessing spread, since it requires the virus to spread from the skin inoculation site to the DRG and back to the skin to produce zosteriform disease. Viruses were scratch inoculated at  $5 \times 10^5$  PFU (Fig. 6A) or  $5 \times 10^4$  PFU (Fig. 6B), and zosteriform disease was scored from days 3 to 7. Inoculation site disease was not different for any of the viruses at  $5 \times 10^5$  or  $5 \times 10^4$  PFU (results not shown). Zosteriform disease scores were also comparable for the three viruses at  $5 \times 10^5$  PFU, while at  $5 \times 10^4$  PFU, NS-gE264 caused slightly less zosteriform disease on days 5 and 6 than did the wild-type and rescue strains, although the differences were not statistically significant (Fig. 6B). Therefore, NS-gE264 causes extensive zosteriform disease, and the flank model can be used to assess whether the HSV-1 Fc $\gamma$ R contributes to virulence.

**The HSV-1 Fc $\gamma$ R blocks IgG Fc-mediated activities in the murine flank model.** HSV-1 IgG antibody is present during recurrent infections but not during the early stages of primary infection. Passive transfer experiments of human IgG antibody to HSV were performed prior to flank challenge to mimic conditions during recurrent infection. The hypothesis was that human IgG antibody to HSV is more active against an Fc $\gamma$ R-negative mutant strain than against wild-type or rescue virus, since activities mediated by the IgG Fc domain will not be blocked by the mutant strain. BALB/c mice were passively immunized with 200  $\mu$ g of human IgG antibody to HSV 20 h prior to infection with NS, rNS-gE264, or NS-gE264. The antibody had no effect on zosteriform disease produced by the wild-type or rescue virus (Fig. 7A); however, the antibody had a dramatic effect on zosteriform disease caused by NS-gE264 (Fig. 7B), while nonimmune human IgG had no effect on any of the strains (Fig. 7A and B). The experiment was repeated by passively immunizing mice with murine IgG antibody to HSV-1 with the expectation that the antibody would have a similar effect on HSV-1 Fc $\gamma$ R-positive and Fc $\gamma$ R-negative strains, since neither virus can block activities mediated by the murine IgG Fc domain (20, 24). Zosteriform disease was reduced in mice passively immunized with murine nonimmune IgG and infected with NS-gE264 compared with rNS-gE264, possibly as a result of the spread defects discussed above; however, the important observation was that murine IgG an-

tibody to HSV-1 had a comparable effect on reducing disease severity for both viruses (Fig. 7C and D).

Mice were passively immunized with 200  $\mu$ g of human IgG antibody to HSV, or nonimmune human IgG as a control, 20 h prior to flank infection and DRG harvested for virus titers to evaluate the contribution of the HSV-1 Fc $\gamma$ R in facilitating virus infection of the DRG. Mice passively immunized with nonimmune human IgG had lower virus titers when infected with NS-gE264 than rNS-gE264 at 3 days postinfection, possibly related to a spread defect of the mutant virus (compare titers of rNS-gE264 NIG with NS-gE264 NIG in Fig. 7E and F); however, the important observation was that human IgG antibody to HSV had no effect on DRG titers of the rescue virus (Fig. 7E), but significantly lowered DRG titers of NS-gE264 on day 3 postinfection (Fig. 7F).

**The HSV-1 Fc $\gamma$ R blocks IgG Fc-mediated activities when antibody is given after the onset of infection.** In humans, HSV IgG antibody is commonly present during recurrent infections as virus travels from the DRG to the site of recurrence. Mice were infected with HSV-1 and antibody was administered 56 h postinfection in an effort to mimic conditions during recurrent infection. Fifty-six hours was chosen based on our preliminary studies (results not shown) and reports by others (51) that demonstrated virus reaches the DRG by that time point.

BALB/c mice were infected by flank inoculation with NS-gE264 or rNS-gE264, and at 56 h postinfection the mice were passively immunized with 200  $\mu$ g of human IgG antibody to HSV or nonimmune human IgG. Extensive zosteriform disease was detected in all mice (results not shown). Previous reports demonstrated that higher titers of antibody are required to modify zosteriform disease if administered after infection; therefore, the experiment was repeated using 2 mg of immune or nonimmune IgG given 56 h postinfection (51). This higher antibody dose was highly effective in reducing zosteriform disease in mice infected with NS-gE264 but had no effect on the rescue virus (Fig. 7G and H). Therefore, the HSV-1 Fc $\gamma$ R provides protection for the virus against antibody in a model that simulates recurrent infection.

**The HSV-1 Fc $\gamma$ R blocks complement-mediated protection and ADCC *in vivo*.** Zosteriform disease was evaluated in complement-sufficient and C3 knockout mice to determine if complement contributes to the reduced zosteriform disease caused by NS-gE264. The C3 knockout mice are in a C57BL/6 background; therefore, C57BL/6 mice were used as controls. A

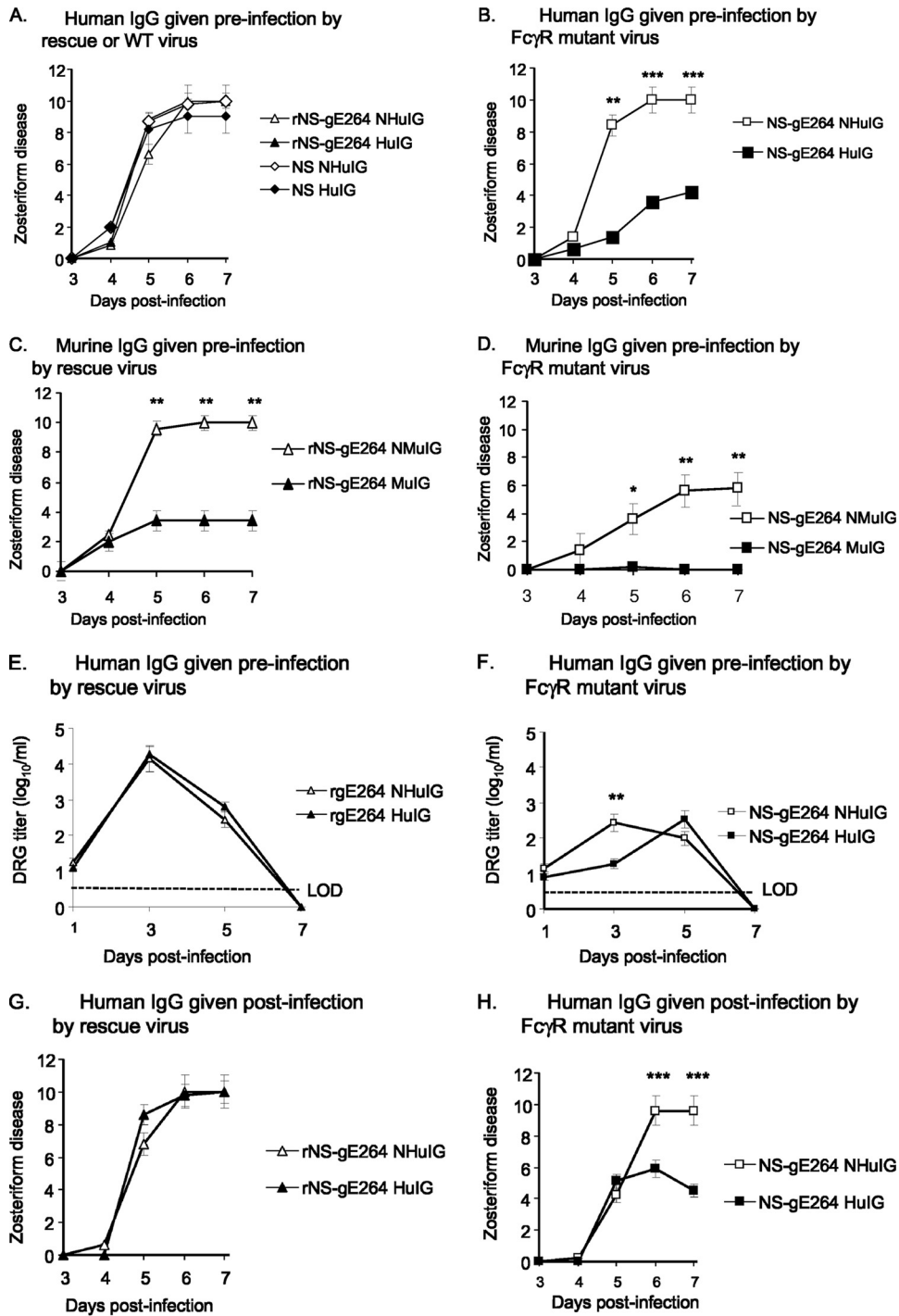


FIG. 7. The HSV-1 FcγR blocks IgG Fc-mediated activities in the murine flank model. (A and B) Mice were passively immunized with 200 μg of human IgG antibody to HSV (human immune globulin [HuIG]) or nonimmune human IgG (NHuIG), and 20 h later they were flank inoculated with  $5 \times 10^5$  PFU of rNS-gE264 or NS (A) or  $5 \times 10^5$  PFU NS-gE264 (B). No differences were detected for the results shown in panel A, while zosteriform disease was significantly lower in the HuIG group on days 5 to 7 in the experiment shown in panel B. Results represent the means and standard deviations of 10 mice per group. (C and D) Mice were passively immunized with 200 μg of murine IgG antibody to HSV-1 (murine immune globulin [MuIG]) or murine nonimmune IgG (NMuIG) and infected with  $5 \times 10^5$  PFU of the rescue strain (C) or  $5 \times 10^5$  PFU of NS-gE264 (D). Zosteriform disease scores in mice that received MuIG were significantly lower than the NMuIG-treated mice on days 5 to 7. Results are the means and standard deviations of 10 animals per group. (E and F) DRG titers in mice passively immunized with 200 μg NHuIG or HuIG and infected with  $5 \times 10^5$  PFU of the rescue virus (E) or  $5 \times 10^5$  PFU of NS-gE264 (F). No difference was detected between NHuIG and HuIG in (E), while a significant difference was detected on day 3 in the experiment shown in panel F. LOD, limit of detection of the assay, which is 2.5 PFU. Results are the means and standard deviations of five animals per group. (G and H) Mice were infected with  $5 \times 10^5$  PFU of the rescue virus (G) or  $5 \times 10^5$  PFU of NS-gE264 (H) and 56 h postinfection were passively immunized with 2 mg of NHuIG or HuIG. No difference was detected in zosteriform disease in animals infected with the rescue virus (G), while significant differences were noted in the NS-gE264 mice on days 6 and 7 postinfection (H). Results are the means and standard deviations of 10 mice per group. \*,  $P < 0.05$ ; \*\*,  $P < 0.01$ ; \*\*\*,  $P < 0.001$ .

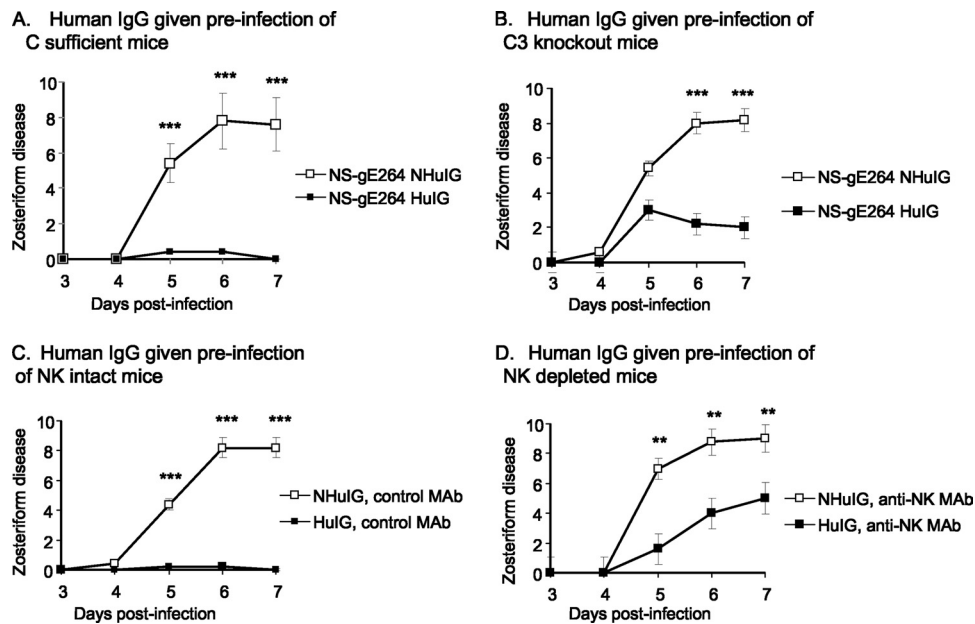


FIG. 8. The HSV-1 Fc $\gamma$ R blocks complement-mediated protection and ADCC. (A) C57BL/6 mice (complement sufficient) were passively immunized with human IgG antibodies to HSV (HuIG) or nonimmune human IgG (NHuIG), and 20 h later they were flank inoculated with  $5 \times 10^6$  PFU of NS-gE264. (B) C3 knockout mice were passively immunized as described for panel A and flank inoculated with  $5 \times 10^5$  PFU of NS-gE264. Results in panels A and B are the means and standard deviations of five mice per group. (C and D) C57BL/6 mice were treated i.p. three times with an isotype control MAb (NK intact mice) (C) or anti-NK MAb PK136 (NK-depleted mice) (D), passively immunized with HuIG or NHuIG, and infected with  $5 \times 10^5$  PFU of NS-gE264. Results in panels C and D are the means and standard deviations of five animals per group. \*\*,  $P < 0.01$ ; \*\*\*,  $P < 0.001$ .

higher-titer inoculum ( $5 \times 10^6$  PFU) was used for these experiments, since C57BL/6 mice are more resistant than BALB/c mice to HSV-1 infection (33, 36). C57BL/6 (complement-sufficient) mice were passively immunized with 200  $\mu$ g of human IgG antibody to HSV or nonimmune human IgG 20 h prior to flank infection with NS-gE264. Animals passively immunized with human IgG antibody to HSV had significantly less zosteriform disease than animals treated with nonimmune human IgG (Fig. 8A), which was similar to results obtained in BALB/c mice (Fig. 7B). The experiment was performed in C3 knockout mice, except a lower inoculation titer was used ( $5 \times 10^5$  PFU) because the animals are partially immunodeficient (8, 28). We postulated that human IgG antibody to HSV would have no effect on zosteriform disease if antibody activity was dependent on complement activation. If complement activation were not required, HSV antibody would be as effective as in complement-sufficient mice.

Zosteriform disease was significantly reduced in mice that received human IgG antibody to HSV (Fig. 8B); however, disease scores were considerably higher than in complement-sufficient mice treated with human IgG antibody to HSV, despite our using a 10-fold-higher inoculum in complement-sufficient mice (Fig. 8A and B, compare human IgG antibody to HSV) ( $P < 0.05$  on days 5 and 6). Therefore, blocking complement activation contributes partially to the protection provided by the HSV-1 Fc $\gamma$ R.

ADCC is primarily mediated by NK cells that express Fc $\gamma$ RIII (CD16) (23). C57BL/6 mice were passively immunized i.p. with 100  $\mu$ g of antibody to deplete NK cells (NK-depleted mice) or with an isotype control (NK-intact mice)

given 1 day prior to infection and 2 and 5 days postinfection. Mice were passively immunized i.p. with human IgG antibody to HSV or nonimmune human IgG and challenged 20 h later by flank inoculation with NS-gE264. The NK-intact mice treated with nonimmune human IgG developed extensive zosteriform disease, while those receiving human IgG antibody to HSV developed minimal disease (Fig. 8C). We postulated that the HSV-1 Fc $\gamma$ R blocks ADCC by binding the Fc domain of human immune IgG; therefore, depleting NK cells should greatly reduce the protection provided by the HSV-1 Fc $\gamma$ R. NK-depleted mice passively immunized with nonimmune human IgG developed extensive zosteriform disease. In contrast, NK-depleted mice treated with human IgG antibody to HSV had considerably more disease than NK-sufficient mice (Fig. 8C and D, compare human IgG antibody to HSV) although less disease than NK-depleted mice treated with nonimmune human IgG (Fig. 8D). Therefore, blocking ADCC mediated by NK cells also partially contributes to the protection provided by the HSV-1 Fc $\gamma$ R.

## DISCUSSION

HSV-1 is not unique among viruses in expressing an Fc $\gamma$ R; however, a role in virulence has only been demonstrated for the HSV-1 Fc $\gamma$ R (34, 42). Other alphaherpesviruses that express an Fc $\gamma$ R include HSV-2, varicella-zoster virus, and pseudorabies virus (19, 20, 25, 26, 32, 44–46, 54). Human cytomegalovirus (CMV) encodes two Fc $\gamma$ Rs, while murine CMV encodes an Fc $\gamma$ R (1, 30). The function of the murine CMV Fc $\gamma$ R in virulence is unclear, since a deletion of the m138 gene



that encodes the Fc $\gamma$ R leads to attenuation of the virus even in the absence of antibody (13). The m138 protein downregulates NK cell ligands from the infected cell surface and the costimulatory molecule B7-1 from the surface of dendritic cells, suggesting that m138 mediates immune evasion independent of its Fc $\gamma$ R activity (29, 41). Hepatitis C virus core antigen has Fc $\gamma$ R activity. Of interest, IgG Fc genotype variants that bind to the viral Fc $\gamma$ R are detected more frequently in patients with persistent HCV infection than in those who clear the virus, suggesting a role for the Fc $\gamma$ R in virulence (37, 43).

Efforts to assess the importance of gE in immune evasion *in vivo* have been hampered by difficulties developing an HSV-1 mutant strain that is intact for spread and axonal targeting but defective in Fc $\gamma$ R activity. We previously reported that NS-gE339 is defective in Fc $\gamma$ R activities; however, that mutant strain produced little zosteriform disease in the mouse flank model, suggesting that NS-gE339 cell-to-cell spread or axonal targeting is impaired (42). Other gE mutant strains include NS-gE210, which is defective in cell-to-cell spread but retains Fc $\gamma$ R activity, and NS-gE380, which is impaired in cell-to-cell spread and Fc $\gamma$ R activity (49). To date, NS-gE264 represents the only gE mutant strain that is defective in Fc $\gamma$ R activity while maintaining sufficient cell-to-cell spread and axonal targeting activity to permit *in vivo* studies of HSV-1 Fc $\gamma$ R function.

Evidence that NS-gE264 is defective in Fc $\gamma$ R activity is based on a previous report (56) that the mutant strain does not form rosettes with IgG-coated erythrocytes, and in two assays reported here. First, NS-gE264 is more susceptible to complement-enhanced antibody neutralization than the rescue strain, indicating that the HSV-1 Fc $\gamma$ R is not blocking complement activation by the Fc domain of human IgG antibody to HSV. Second, flow cytometry demonstrates decreased binding of nonimmune human IgG to HSV-1-infected cells. Binding of the Fc domain of nonimmune IgG to the HSV-1 Fc $\gamma$ R requires intact gE sequences and formation of a complex between gE and gI at the infected cell surface (17). NS-gE264 forms a gE/gI complex, as demonstrated by coimmunoprecipitation of gE and gI from infected cells. The slightly reduced expression of gE at the surface of NS-gE264-infected cells is consistent with the Western blot results, that showed underglycosylation of gE and gI, suggesting a possible defect in gE and gI trafficking from the endoplasmic reticulum to the Golgi complex and cell surface. However, the modest reduction in gE expression is not sufficient to account for the marked decrease in IgG Fc binding, which is best attributed to altered binding to gE.

The observation reported here that the mutation in gE264 does not disrupt the gE/gI complex differs from our prior report, in which gE/gI failed to coimmunoprecipitate from cells transfected with plasmids expressing gE264 and gI (2). Subsequent work by others showed that the HSV-1 gE N-terminal 188 amino acids are sufficient for gE/gI complex formation (48). The crystal structure of gE/gI bound to IgG Fc also suggests that residues near gE amino acid 264 are not required for gE/gI complex formation (53). The observation that gE and gI form a complex in NS-gE264 but not in cells transfected with plasmids expressing gE264 and gI may reflect differences between transfected and infected cells, or differences in antibodies used for immunoprecipitation. In the present study, gI MAb Fd69 was used, while Basu et al. used gI MAb 3104,

which may interfere with the complex formed between gE264 and gI (2).

The NS-gE264 strain is partially impaired in epithelial cell-to-cell spread, based on its forming small plaques in HaCaT cells, similar to observations reported by others (47). This cell-to-cell spread phenotype may be explained partly by the slightly reduced expression of gE at the surface of NS-gE264-infected cells, or by the altered glycosylation pattern of gE and gI detected by Western blotting. However, NS-gE264 epithelial cell-to-axon spread was not impaired as determined by using SCG neuron cultures. The mouse retina infection model was used to further assess the NS-gE264 spread phenotype *in vivo*. The results demonstrated a partial impairment in cell-to-cell spread in the mouse retina based on the approximate number of immunofluorescent cells. Previously we reported that NS-gE264 antigens were detected in the optic nerve (56). Here we report that NS-gE264 antigens are also detected in regions of the brain that require intact anterograde spread from the optic nerve; however, antigens were present at reduced levels compared with the rescue strain. Retrograde spread was evaluated by antigen detection in specific brain nuclei, with only slight reductions noted in retrograde spread. Importantly, the spread phenotype of NS-gE264 was only minimally impaired in the mouse flank model. The fact that NS-gE264 caused extensive zosteriform disease enabled us to evaluate the function of the HSV-1 Fc $\gamma$ R without confounding the results because of impaired spread.

The HSV-1 Fc $\gamma$ R blocks antibody functions mediated by the IgG Fc domain; therefore, its immune evasion activities are relevant in recurrent infections. The zosteriform infection model was selected since the pathway traveled by the virus from the DRG to the skin is similar to the pathway traveled during recurrent infections in humans. The Fc domain of murine IgG does not bind to the HSV-1 Fc $\gamma$ R; therefore, to assess Fc $\gamma$ R activity we passively immunized mice with human IgG antibody to HSV. When antibody is injected prior to infection, the model assesses the role of the HSV-1 Fc $\gamma$ R in evading antibody that is produced by immunization or in newborns, in whom HSV IgG is passively transferred from mother to baby. When antibody is given after infection, the model addresses the contribution of the HSV-1 Fc $\gamma$ R during recurrent infections.

Passive immunization with human IgG antibody to HSV prior to infection had no impact on zosteriform disease caused by the wild-type and rescue viruses. In contrast, zosteriform disease scores were significantly reduced by human IgG antibody to HSV in mice infected with the HSV-1 Fc $\gamma$ R mutant strain, while nonimmune human IgG had no effect. When murine IgG antibody to HSV-1 was administered, disease scores of rescue and Fc $\gamma$ R mutant strains were both reduced, which supports the conclusion that the HSV-1 Fc $\gamma$ R blocks activities mediated by the IgG Fc domain of human, but not murine, antibody. Virus titers in the DRG were significantly reduced in mice infected with NS-gE264 and passively immunized with human IgG antibody to HSV, compared with those treated with nonimmune human IgG at 3 days postinfection, although by 5 days the titers were not different. These results suggest that by delaying the time it takes virus to infect the DRG, other host defenses may have sufficient time to mount

an effective immune response to reduce the severity of zosteriform infection.

The HSV-1 Fc $\gamma$ R may also protect the virus from antibody as the virus exits axons in the skin. To better assess this stage of infection, human IgG antibody to HSV was administered at 56 h postinfection, after the virus had reached the DRG. Higher antibody titers were required to demonstrate an effect on zosteriform disease when administered after infection; however, the results clearly demonstrated that the HSV-1 Fc $\gamma$ R reduces the effectiveness of antibody at this later stage of infection.

*In vitro* studies demonstrate that the HSV-1 Fc $\gamma$ R protects the virus and infected cells from complement-enhanced antibody neutralization and ADCC (18, 20). Experiments were performed in C3 knockout mice or NK cell-depleted mice to assess the importance of the HSV-1 Fc $\gamma$ R in blocking IgG Fc-mediated complement activation and ADCC *in vivo*. Zosteriform disease was partially reduced in NS-gE264-infected mice passively immunized with human IgG antibody to HSV, indicating that complement is not the only host defense factor interacting with the IgG Fc domain. We reached a similar conclusion when assessing ADCC, since preventing ADCC by depleting NK cells did not totally explain the protection provided by the HSV-1 Fc $\gamma$ R. Therefore, the HSV-1 Fc $\gamma$ R blocks the interaction of both complement and NK cells with the IgG Fc domain.

#### ACKNOWLEDGMENTS

NC-1 serum was provided by G. H. Cohen and R. J. Eisenberg, University of Pennsylvania.

This work was supported by NIH grants HL 028220 and AI 033063.

#### REFERENCES

- Atalay, R., et al. 2002. Identification and expression of human cytomegalovirus transcription units coding for two distinct Fc $\gamma$  receptor homologs. *J. Virol.* **76**:8596–8608.
- Basu, S., G. Dubin, M. Basu, V. Nguyen, and H. M. Friedman. 1995. Characterization of regions of herpes simplex virus type 1 glycoprotein E involved in binding the Fc domain of monomeric IgG and in forming a complex with glycoprotein I. *J. Immunol.* **154**:260–267.
- Basu, S., et al. 1997. Mapping regions of herpes simplex virus type 1 glycoprotein I required for formation of the viral Fc receptor for monomeric IgG. *J. Immunology* **158**:209–215.
- Baucke, R. B., and P. G. Spear. 1979. Membrane proteins specified by herpes simplex viruses. V. Identification of an Fc-binding glycoprotein. *J. Virol.* **32**:779–789.
- Bell, S., M. Cranage, L. Borysiewicz, and T. Minson. 1990. Induction of immunoglobulin G Fc receptors by recombinant vaccinia viruses expressing glycoproteins E and I of herpes simplex virus type 1. *J. Virol.* **64**:2181–2186.
- Berman, E. J., and J. M. Hill. 1985. Spontaneous ocular shedding of HSV-1 in latently infected rabbits. *Invest. Ophthalmol. Vis. Sci.* **26**:587–590.
- Brittle, E. E., F. Wang, J. M. Lubinski, R. M. Bunte, and H. M. Friedman. 2008. A replication-competent, neuronal spread-defective, live attenuated herpes simplex virus type 1 vaccine. *J. Virol.* **82**:8431–8441.
- Carroll, M. C. 2000. The role of complement in B cell activation and tolerance. *Adv. Immunol.* **74**:61–88.
- Chapman, T. L., et al. 1999. Characterization of the interaction between the herpes simplex virus type 1 Fc receptor and immunoglobulin G. *J. Biol. Chem.* **274**:6911–6919.
- Ch'ng, T. H., E. A. Flood, and L. W. Enquist. 2005. Culturing primary and transformed neuronal cells for studying pseudorabies virus infection. *Methods Mol. Biol.* **292**:299–316.
- Ch'ng, T. H., and L. W. Enquist. 2005. Neuron-to-cell spread of pseudorabies virus in a compartmented neuronal culture system. *J. Virol.* **79**:10875–10889.
- Cohen, G. H., et al. 1980. Structural analysis of the capsid polypeptides of herpes simplex virus types 1 and 2. *J. Virol.* **34**:521–531.
- Crnkovic-Mertens, I., et al. 1998. Virus attenuation after deletion of the cytomegalovirus Fc receptor gene is not due to antibody control. *J. Virol.* **72**:1377–1382.
- Dingwell, K. S., et al. 1994. Herpes simplex virus glycoproteins E and I facilitate cell-to-cell spread *in vivo* and across junctions of cultured cells. *J. Virol.* **68**:834–845.
- Dingwell, K. S., L. C. Doering, and D. C. Johnson. 1995. Glycoproteins E and I facilitate neuron-to-neuron spread of herpes simplex virus. *J. Virol.* **69**:7087–7098.
- Dubin, G., et al. 1994. Characterization of domains of herpes simplex virus type 1 glycoprotein E involved in Fc binding activity for immunoglobulin G aggregates. *J. Virol.* **68**:2478–2485.
- Dubin, G., I. Frank, and H. M. Friedman. 1990. Herpes simplex virus type 1 encodes two Fc receptors which have different binding characteristics for monomeric immunoglobulin G (IgG) and IgG complexes. *J. Virol.* **64**:2725–2731.
- Dubin, G., E. Socolof, I. Frank, and H. M. Friedman. 1991. Herpes simplex virus type 1 Fc receptor protects infected cells from antibody-dependent cellular cytotoxicity. *J. Virol.* **65**:7046–7050.
- Favoreel, H. W., H. J. Nauwynck, P. Van Oostveldt, T. C. Mettenleiter, and M. B. Pensaert. 1997. Antibody-induced and cytoskeleton-mediated redistribution and shedding of viral glycoproteins, expressed on pseudorabies virus-infected cells. *J. Virol.* **71**:8254–8261.
- Frank, I., and H. M. Friedman. 1989. A novel function of the herpes simplex virus type 1 Fc receptor: participation in bipolar bridging of antiviral immunoglobulin G. *J. Virol.* **63**:4479–4488.
- Friedman, H. M., E. J. Macarak, R. R. MacGregor, J. Wolfe, and N. A. Kefalides. 1981. Virus infection of endothelial cells. *J. Infect. Dis.* **143**:266–273.
- Hook, L. M., J. Huang, M. Jiang, R. Hodinka, and H. M. Friedman. 2008. Blocking antibody access to neutralizing domains on glycoproteins involved in entry as a novel mechanism of immune evasion by herpes simplex virus type 1 glycoproteins C and E. *J. Virol.* **82**:6935–6941.
- Janeway, C. A., P. Travers, M. Walport, and J. D. Capra. 1999. Immunobiology. The immune system in health and disease, 4th ed. Elsevier Science Ltd./Garland Publishing, New York, NY.
- Johansson, P. J., E. B. Myhre, and J. Blomberg. 1985. Specificity of Fc receptors induced by herpes simplex virus type 1: comparison of immunoglobulin G from different animal species. *J. Virol.* **56**:489–494.
- Johnson, D. C., and V. Feenstra. 1987. Identification of a novel herpes simplex virus type 1-induced glycoprotein which complexes with gE and binds immunoglobulin. *J. Virol.* **61**:2208–2216.
- Johnson, D. C., M. C. Frame, M. W. Ligas, A. M. Cross, and N. D. Stow. 1988. Herpes simplex virus immunoglobulin G Fc receptor activity depends on a complex of two viral glycoproteins, gE and gI. *J. Virol.* **62**:1347–1354.
- Kitaichi, N., et al. 2002. Diminution of experimental autoimmune uveoretinitis (EAU) in mice depleted of NK cells. *J. Leukoc. Biol.* **72**:1117–1121.
- Kopf, M., B. Abel, A. Gallimore, M. Carroll, and M. F. Bachmann. 2002. Complement component C3 promotes T-cell priming and lung migration to control acute influenza virus infection. *Nat. Med.* **8**:373–378.
- Lenac, T., et al. 2006. The herpesviral Fc receptor FcR-1 down-regulates the NK2D2 ligands MULT-1 and H60. *J. Exp. Med.* **203**:1843–1850.
- Lilley, B. N., H. L. Ploegh, and R. S. Tirabassi. 2001. Human cytomegalovirus open reading frame TRL11/IRL11 encodes an immunoglobulin G Fc-binding protein. *J. Virol.* **75**:11218–11221.
- Lin, X., J. M. Lubinski, and H. M. Friedman. 2004. Immunization strategies to block the herpes simplex virus type 1 immunoglobulin G Fc receptor. *J. Virol.* **78**:2562–2571.
- Litwin, V., W. Jackson, and C. Grose. 1992. Receptor properties of two varicella-zoster virus glycoproteins, gpI and gpIV, homologous to herpes simplex virus gE and gI. *J. Virol.* **66**:3643–3651.
- Lopez, C. 1975. Genetics of natural resistance to herpesvirus infections in mice. *Nature* **258**:152–153.
- Lubinski, J. M., et al. 2002. Herpes simplex virus type 1 evades the effects of antibody and complement *in vivo*. *J. Virol.* **76**:9232–9241.
- Lubinski, J. M., et al. 1998. Herpes simplex virus type 1 glycoprotein gC mediates immune evasion *in vivo*. *J. Virol.* **72**:8257–8263.
- Lundberg, P., et al. 2003. A locus on mouse chromosome 6 that determines resistance to herpes simplex virus also influences reactivation, while an unlinked locus augments resistance of female mice. *J. Virol.* **77**:11661–11673.
- Maillard, P., et al. 2004. Fc $\gamma$  receptor-like activity of hepatitis C virus core protein. *J. Biol. Chem.* **279**:2430–2437.
- McGraw, H. M., S. Awasthi, J. A. Wojcechowskyj, and H. M. Friedman. 2009. Anterograde spread of herpes simplex virus type 1 requires glycoprotein E and glycoprotein I but not Us9. *J. Virol.* **83**:8315–8326.
- McGraw, H. M., and H. M. Friedman. 2009. Herpes simplex virus type 1 glycoprotein E mediates retrograde spread from epithelial cells to neurites. *J. Virol.* **83**:4791–4799.
- Metcalf, J. F., S. Chatterjee, J. Koga, and R. J. Whitley. 1988. Protection against herpetic ocular disease by immunotherapy with monoclonal antibodies to herpes simplex virus glycoproteins. *Intervirology* **29**:39–49.
- Mintern, J. D., et al. 2006. Viral interference with B7-1 costimulation: a new role for murine cytomegalovirus Fc receptor-1. *J. Immunol.* **177**:8422–8431.
- Nagashunmugam, T., et al. 1998. *In vivo* immune evasion mediated by the

- herpes simplex virus type 1 immunoglobulin G Fc receptor. *J. Virol.* **72**:5351–5359.
43. **Pandey, J. P., et al.** 2008. Genetic markers of IgG influence the outcome of infection with hepatitis C virus. *J. Infect. Dis.* **198**:1334–1336.
44. **Para, M. F., R. B. Baucke, and P. G. Spear.** 1982. Glycoprotein gE of herpes simplex virus type 1: effects of anti-gE on virion infectivity and on virus-induced Fc-binding receptors. *J. Virol.* **41**:129–136.
45. **Para, M. F., R. B. Baucke, and P. G. Spear.** 1980. Immunoglobulin G (Fc)-binding receptors on virions of herpes simplex virus type 1 and transfer of these receptors to the cell surface by infection. *J. Virol.* **34**:512–520.
46. **Para, M. F., L. Goldstein, and P. G. Spear.** 1982. Similarities and differences in the Fc-binding glycoprotein (gE) of herpes simplex virus types 1 and 2 and tentative mapping of the viral gene for this glycoprotein. *J. Virol.* **41**:137–144.
47. **Polcicova, K., K. Goldsmith, B. L. Rainish, T. W. Wisner, and D. C. Johnson.** 2005. The extracellular domain of herpes simplex virus gE is indispensable for efficient cell-to-cell spread: evidence for gE/gI receptors. *J. Virol.* **79**:11990–12001.
48. **Rizvi, S. M., and M. Raghavan.** 2001. An N-terminal domain of herpes simplex virus type Ig E is capable of forming stable complexes with gI. *J. Virol.* **75**:11897–11901.
49. **Saldanha, C. E., et al.** 2000. Herpes simplex virus type 1 glycoprotein E domains involved in virus spread and disease. *J. Virol.* **74**:6712–6719.
50. **Sen, D. K., and G. S. Sarin.** 1979. Immunoglobulin concentrations in human tears in ocular diseases. *Br. J. Ophthalmol.* **63**:297–300.
51. **Simmons, A., and A. A. Nash.** 1985. Role of antibody in primary and recurrent herpes simplex virus infection. *J. Virol.* **53**:944–948.
52. **Simova, J., J. Bubenik, J. Bieblova, and T. Jandlova.** 2004. The role of NK1.1+ cells in the protection against MHC class I+ HPV16-associated tumours. *Folia Biol. (Praha)* **50**:200–202.
53. **Sprague, E. R., C. Wang, D. Baker, and P. J. Bjorkman.** 2006. Crystal structure of the HSV-1 Fc receptor bound to Fc reveals a mechanism for antibody bipolar bridging. *PLoS Biol.* **4**:e148.
54. **Van de Walle, G. R., H. W. Favoreel, H. J. Nauwynck, and M. B. Pensaert.** 2003. Antibody-induced internalization of viral glycoproteins and gE-gI Fc receptor activity protect pseudorabies virus-infected monocytes from efficient complement-mediated lysis. *J. Gen. Virol.* **84**:939–947.
55. **Van Vliet, K. E., L. A. De Graaf-Miltenburg, J. Verhoef, and J. A. Van Strijp.** 1992. Direct evidence for antibody bipolar bridging on herpes simplex virus-infected cells. *Immunology* **77**:109–115.
56. **Wang, F., et al.** 2005. Herpes simplex virus type 1 glycoprotein E is required for axonal localization of capsid, tegument, and membrane glycoproteins. *J. Virol.* **79**:13362–13372.
57. **Watkins, J. F.** 1964. Adsorption of sensitized sheep erythrocytes to HeLa cells infected with herpes simplex virus. *Nature* **202**:1364–1365.
58. **Weeks, B. S., P. Sundaresan, T. Nagashunmugam, E. Kang, and H. M. Friedman.** 1997. The herpes simplex virus-1 glycoprotein E (gE) mediates IgG binding and cell-to-cell spread through distinct gE domains. *Biochem. Biophys. Res. Commun.* **235**:31–35.